SUPPLEMENTARY FIGURE LEGENDS

Supplementary Figure 1: Loss of C9ORF72 function suppresses neurite outgrowth of motor neurons.

(a) Schematic of production of Hb9::GFP+ motor neurons derived from mouse embryonic stem cells, subsequent ASO-mediated suppression of endogenous C9ORF72 expression, and assessment of neurite outgrowth.

(b) *C9orf72* RNA expression in mouse ESC-derived cells following 2 weeks of ASO treatment. Error bars represent SEM (n = 3 per group). Statistical evaluations were performed using student's *t*-test, unpaired, two-tailed.

(c) Quantification of neurite outgrowth of enriched mouse ESC-derived motor neurons after 2 weeks of ASO treatment. Error bars represent SEM (n = 5 per group). Statistical evaluations were performed using student's *t*-test, unpaired, two-tailed.

Supplementary Figure 2 (Related to Figure 1): Age-dependent C9ORF72 dipeptide-repeat protein accumulation in brain regions of mice expressing 66 GGGGCC repeats.

(a) 66-repeat-containing *C9orf72* RNAs in cortex, cerebellum, spinal cord, and spleen of 2-week-old wild type mice post intracerebroventricular injection of C9 AAV at P0. Error bars represent SEM (n = 3 animals per group). Statistical significance was evaluated using one-way ANOVA with Tukey's post hoc test.

(b) 66-repeat-containing *C9orf72* RNA expression (post intracerebroventricular injection of C9 AAV at P0) in the cortex of 3-month-old mice with neither, one or both endogenous *C9orf72* alleles inactivated. Error bars represent SEM (n = 4 animals per group).

(c) Spleen weight at 9 months of age for mice with indicated genotypes. Error bars represent SEM (n = 4 $C9^{2R}$,$C9orf72^{+/+}$, n = 4 $C9^{2R}$,$C9orf72^{+/-}$, n = 4 $C9^{2R}$,$C9orf72^{-/-}$; n = 6 $C9^{66R}$,$C9orf72^{+/+}$, n = 4 $C9^{66R}$,$C9orf72^{+/-}$, n = 3 $C9^{66R}$,$C9orf72^{-/-}$). Statistical significance was evaluated using one-way ANOVA with Tukey's post hoc test.

(d-e) Levels of poly(GP) **(d)** or poly(GA) **(e)** measured by immunoassay in the cortical extracts of 3- and 10-month-old mice with normal, reduced or absence of endogenous C9ORF72. Error bars represent SEM (for 3-month-old animals, n = 4 $C9^{66R}$,$C9orf72^{+/+}$, n = 4 $C9^{66R}$,$C9orf72^{+/-}$, n = 4 $C9^{66R}$,$C9orf72^{-/-}$; for 10-month-old animals, n = 3 $C9^{66R}$,$C9orf72^{+/+}$, n = 3 $C9^{66R}$,$C9orf72^{+/-}$, n = 4 $C9^{66R}$,$C9orf72^{-/-}$). Between different groups of genotypes, statistical evaluations were performed using one-way ANOVA with Tukey's post hoc test. Between different groups of ages within the same genotype, statistical evaluations were performed using student's *t*-test, unpaired, two-tailed.

Supplementary Figure 3 (Related to Figure 2): No detectable expression of a predicted C9ORF72 short isoform in human cortex.

(*Three lanes at the left*) Immunoblotting with antibodies generated against the human C9ORF72 amino terminus (amino acids 1-169) to detect the full length and predicted short isoform C9ORF72 proteins in human cortex from three neurologically normal donors. (*Five lanes at the right*) The detection limit for the predicted 25 kD short isoform C9ORF72 was determined by immunoblotting of a dilution series of a recombinant 25 kD isoform of C9ORF72 (diluted into mouse cortical extract from *C9orf72*$^{-/-}$ mice). Two independent experiments were performed with similar results.

Supplementary Figure 4 (Related to Figure 3): ALS and FTD-associated behavioral assessment in $C9^{450C}$ transgenic mice with neither, one or both endogenous *C9orf72* alleles inactivated.

(a-d) Behavioral performances in *C9ORF72* transgenic mice with normal, reduced, or absence of endogenous C9ORF72 (n = 49 Non-Tg, n = 28 $C9^{450C}$, n = 15 $C9^{450C}$,$C9orf72^{+/-}$, n = 12 $C9^{450C}$,$C9orf72^{-/-}$, n = 25 $C9orf72^{+/-}$, n = 25 $C9orf72^{-/-}$) at 12 months of age. Error bars represent SEM. Statistical evaluations were performed using one-way ANOVA with Tukey's post hoc test. n.s., not significant.

(a) Whole body weights at 12 months of age for each indicated genotype.

(b) Hindlimb weakness measured by grip-strength assay.

(c) Stride length of the front and hind limbs measured by gait analysis.

(d) Spontaneous locomotor activity determined in an open field by the number of beam breaks in every 5 minutes session of a 60 minute-trial.

Supplementary Figure 5 (Related to Figure 4): No significant axonal pathology or glial activation in spinal cords of C9^{450C} transgenic mice with normal, reduced, or absence of endogenous C9ORF72.

(a) Quantification of spinal motor neuron area at 12 months of age. Each solid dot represents a single lumbar spinal motor neuron. Error bars represent SEM (n = 3 Non-Tg, n = 2 C9^{450C}, n = 2 C9^{450C},*C9orf72*$^{+/-}$, n = 3 C9^{450C},*C9orf72*$^{-/-}$).

(b) Quantification of total motor axons in the lumbar L5 motor root at 12 months of age. Error bars represent SEM (n = 5 Non-Tg, n = 3 C9^{450C}, n = 3 C9^{450C},*C9orf72*$^{+/-}$, n = 3 C9^{450C},*C9orf72*$^{-/-}$, n = 4 *C9orf72*$^{+/-}$, n = 4 *C9orf72*$^{-/-}$).

(c) Representative images of motor axons in the lumbar L5 motor root at 12 months of age.

(d) Distribution of L5 motor axon diameters at 12 months of age. Error bars represent SEM (n = 5 Non-Tg, n = 3 C9^{450C}, n = 3 C9^{450C},*C9orf72*$^{+/-}$, n = 3 C9^{450C},*C9orf72*$^{-/-}$, n = 4 *C9orf72*$^{+/-}$, n = 4 *C9orf72*$^{-/-}$).

(e) Immunofluorescence staining with antibodies recognizing (*upper panels*) the microglial marker Iba-1 and (*lower panels*) the astrocytic marker GFAP in lumbar spinal cord sections of 12-month-old *C9orf72* transgenic mice with normal, reduced, or absence of endogenous C9ORF72. (*Upper and lower rightmost images*) Analyses of spinal cord sections from end-stage 14-month-old transgenic mice expressing ALS-causing mutant SOD1^{G37R}. In all images, dashed outlines correspond to the boundary between the gray and white matter. Experiment was reproduced three times independently with similar results.

(f) Levels of poly(GP) by immunoassay in the cortex of $C9^{450C}$ and wild type mice expressing 66 repeats at 10 months of age. Error bars represent SEM (n = 3 $C9^{66R}$,*C9orf72*$^{+/+}$, n = 5 $C9^{450C}$,*C9orf72*$^{+/+}$). Statistical significance was evaluated using Student's *t*-test, unpaired, two-tailed.

Supplementary Figure 6 (Related to Figure 5): Loss of C9ORF72 function inhibits autophagy *in vitro*.

(a-b) Immunoblotting analysis of LC3 (**a**) in extracts of mouse ear fibroblast (MEF) cells from adult *C9orf72* mice with normal, reduced or absence of C9ORF72. MEF cells were kept under basal growth conditions or treated for 2 hours with bafilomycin (30 μM) or rapamycin (200 nM). Quantification of LC3B-II accumulated levels were normalized to actin **(b)**. Error bars represent SEM of three measurements from three independent experiments. Statistical analyses were performed using two-way ANOVA with Tukey's post hoc test.

(c-d) Immunoblotting analyses for the autophagic marker LC3 **(c)** and p62 **(d)** in cortical extracts from 6-month-old mice with normal, reduced or absence of C9ORF72. Actin was used as a loading control. Experiment was reproduced three times independently with similar results.

(e) Immunoblotting analyses of cortical extracts from 6-month-old non-transgenic or $C9^{450C}$ transgenic mice with normal, reduced or loss of C9ORF72 with antibodies against ubiquitin. Actin was used as a loading control. Experiment was reproduced two times independently with similar results.

Supplementary Figure 7: Proposed synergy between gain-of-toxic function (GOF) and loss of function (LOF) from ALS/FTD-linked repeat expansions in *C9orf72* exacerbates accumulation of poly-dipeptide repeat proteins and cellular toxicity.

Supplementary Figure 8: Scans of immunoblots presented in the current study.

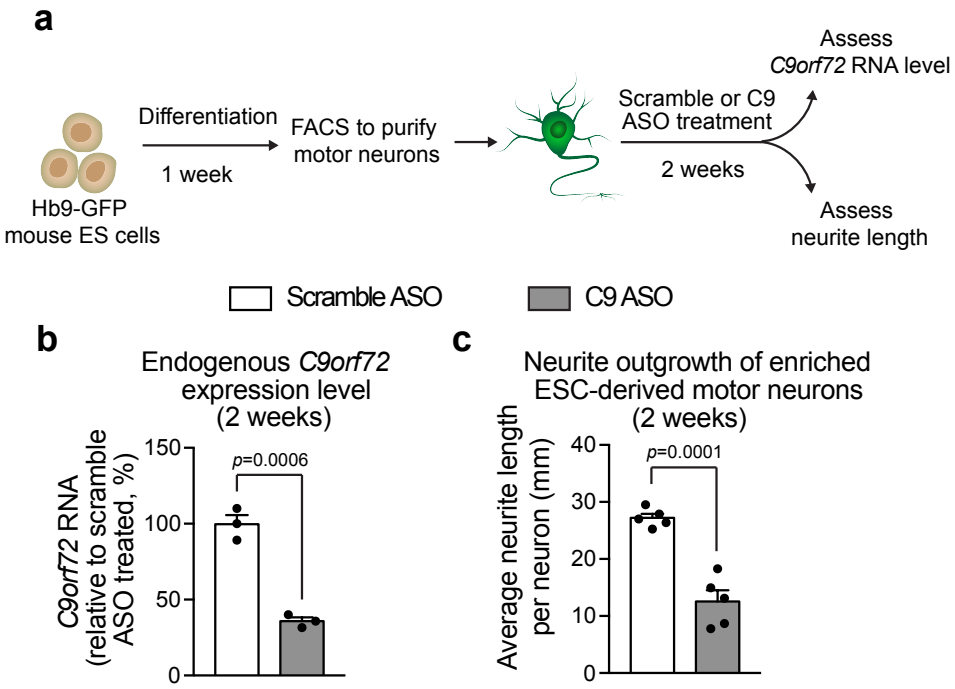

Supplementary Figure 1: Loss of C9ORF72 function suppresses neurite outgrowth of motor neurons.

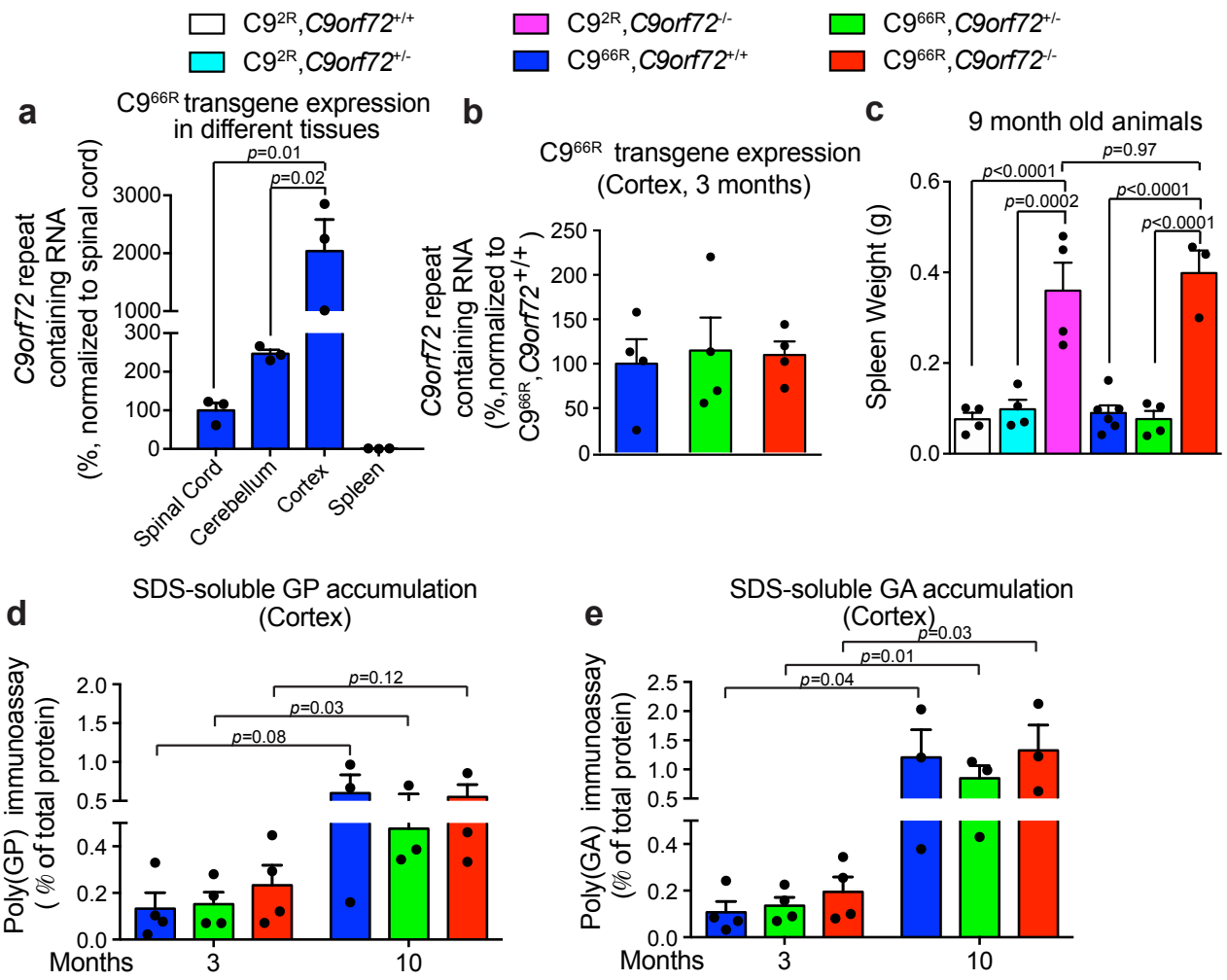

Supplementary Figure 2 (Related to Figure 1): Age-dependent C9ORF72 dipeptide-repeat protein accumulation in brain regions of mice expressing 66 GGGGCC repeats.

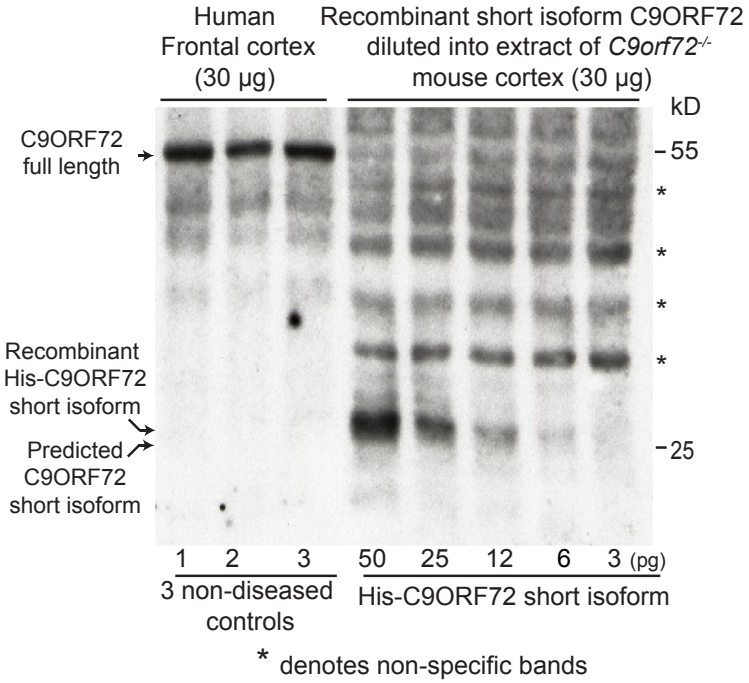

Supplementary Figure 3 (Related to Figure 2): No detectable expression of a predicted C9ORF72 short isoform in human cortex.

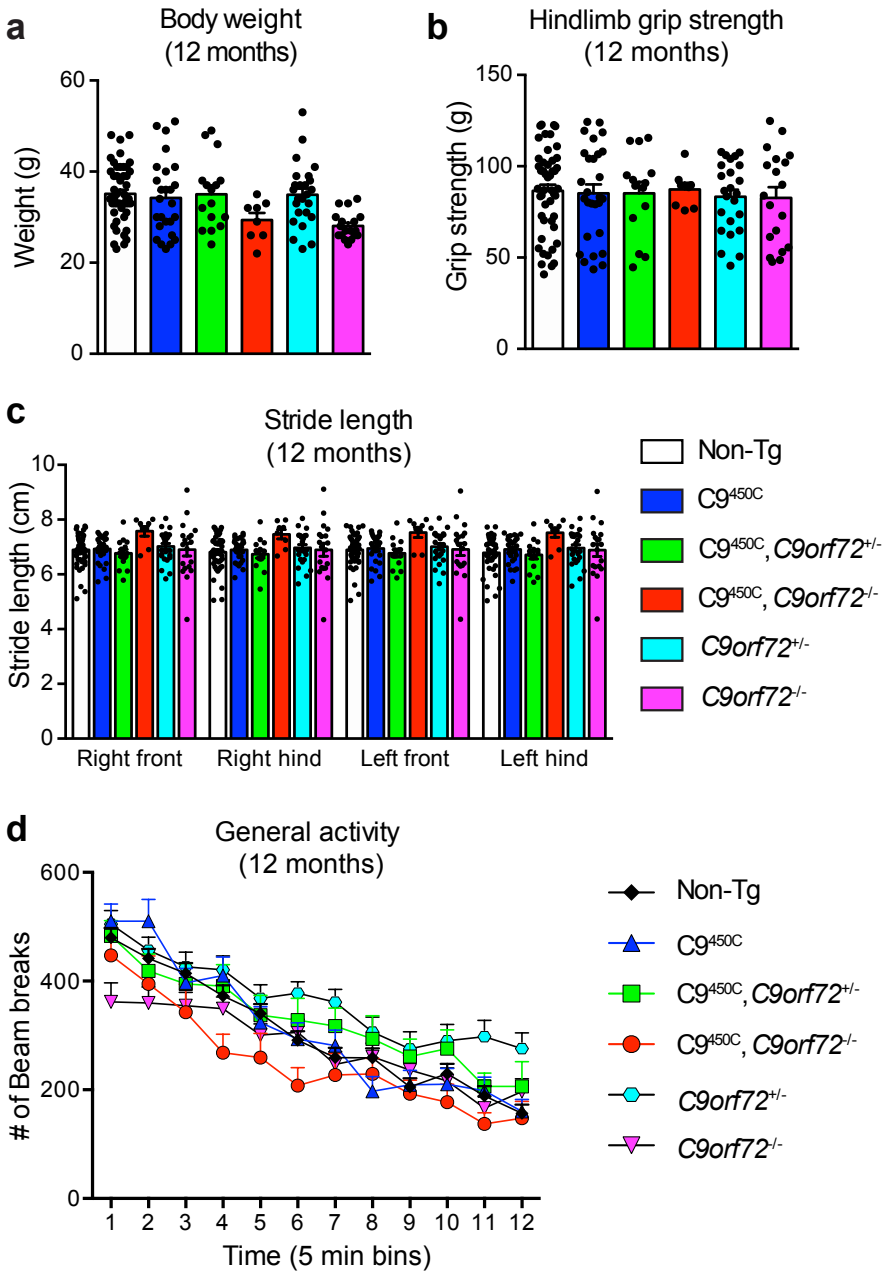

Supplementary Figure 4 (Related to Figure 3): ALS and FTD-associated behavioral assessment in C9^{450C} transgenic mice with neither, one or both endogenous *C9orf72* alleles inactivated.

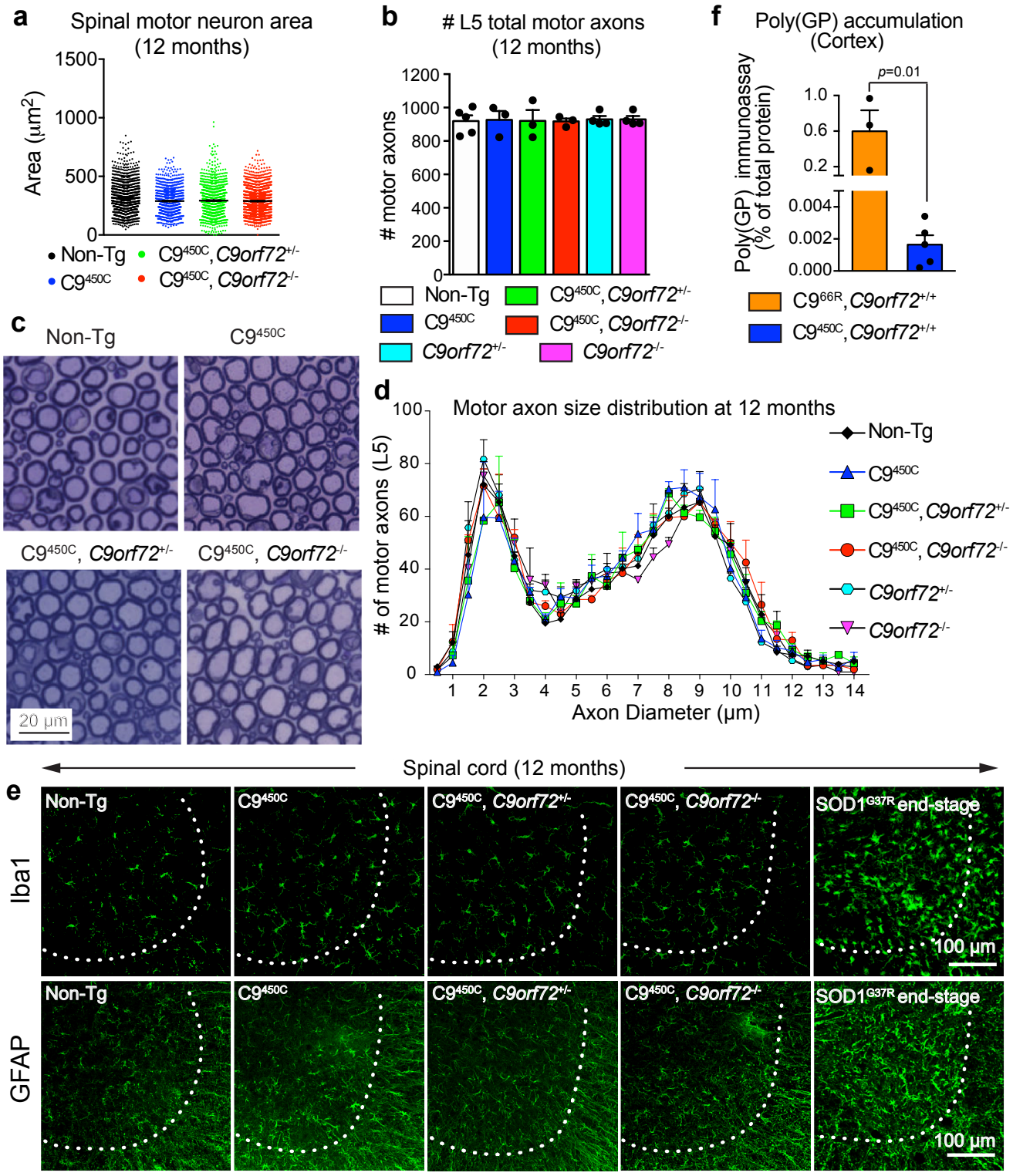

Supplemental Figure 5 (Related to Figure 4): No significant axonal pathology or glial activation in spinal cords of C9^{450C} transgenic mice in the presence or absence of endogenous C9ORF72.

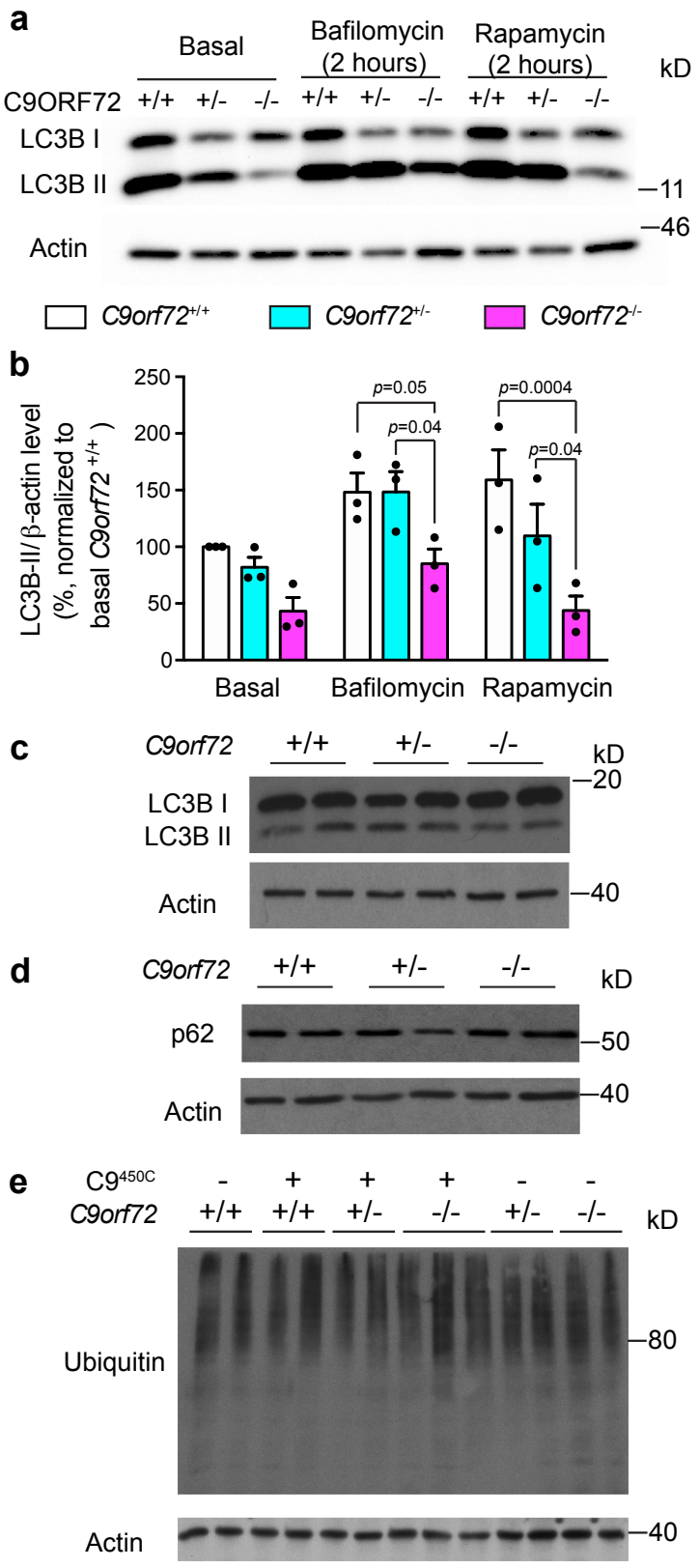

Supplementary Figure 6 (Related to Figure 5): Reduction or absence of C9ORF72 inhibits autophagy *in vitro*.

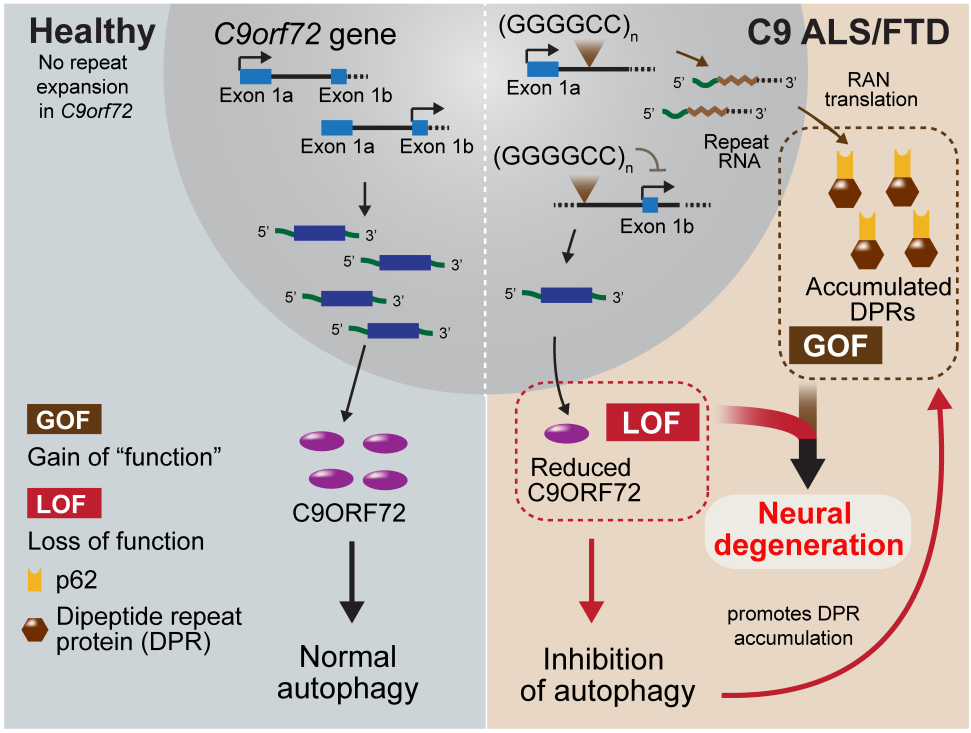

Supplementary Figure 7: Proposed synergy between gain-of-toxic function (GOF) and loss of function (LOF) from ALS/FTD-linked repeat expansions in *C9orf72* exacerbates accumulation of poly-dipeptides repeat proteins and cellular toxicity.

Supplementary Figure 6a

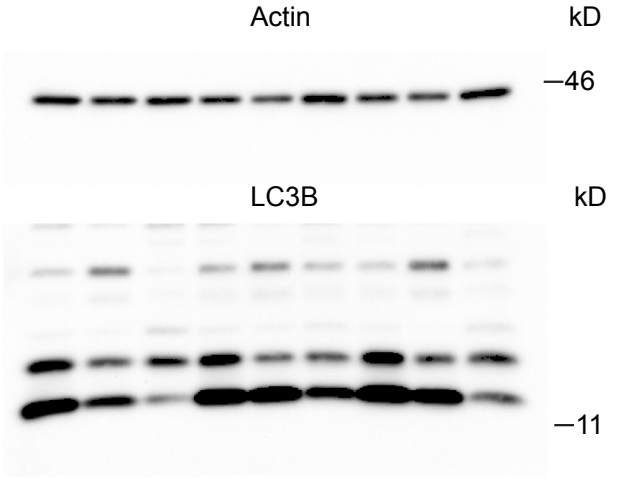

Supplementary Figure 6c

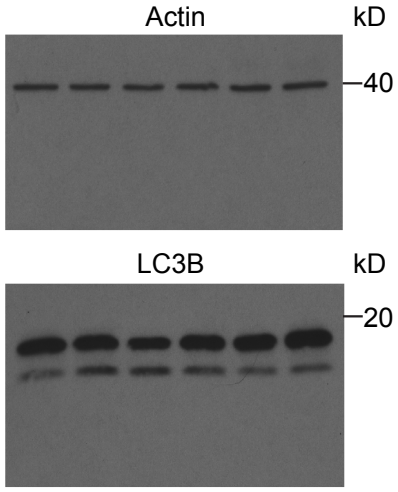

Supplementary Figure 6d

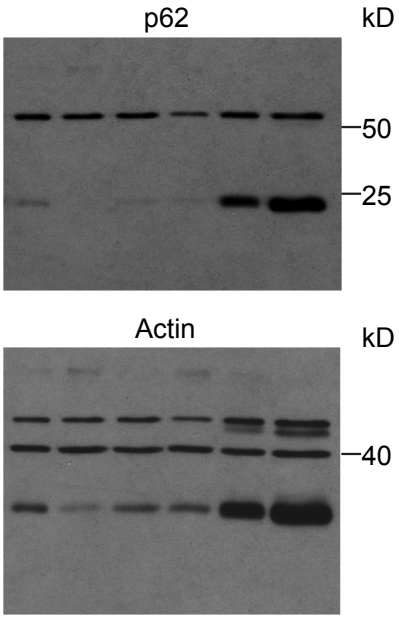

Supplementary Figure 6e

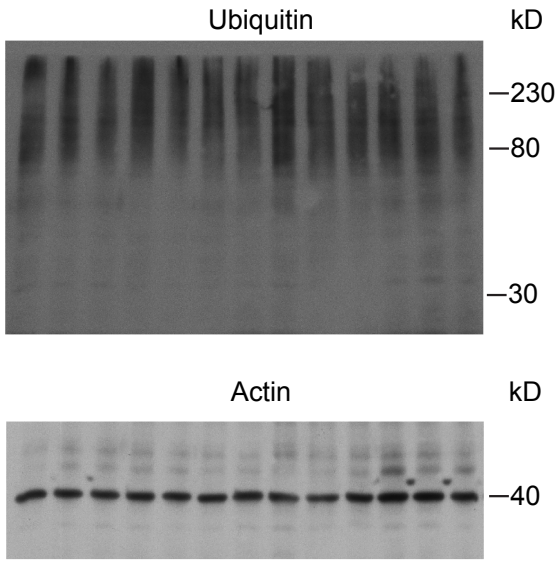

Supplementary Figure 8: Scans of immunoblots presented in the current study.